Turkish Journal of Electrical Engineering & Computer Sciences

http://journals.tubitak.gov.tr/elektrik/

Research Article

Turk J Elec Eng & Comp Sci
(2016) 24: 3621 – 3637

doi:10.3906/elk-1407-21

A current-based simple analog MPPT circuit for PV systems

Bülent BÜYÜKGÜZEL, Murat AKSOY*
Department of Electrical & Electronics Engineering, Çukurova University, Adana, Turkey

Received: 03.07.2014 • **Accepted/Published Online:** 20.05.2015 • **Final Version:** 20.06.2016

Abstract: A new single pilot-sensor maximum power point tracking (MPPT) system, consisting of a buck type DC/DC converter, was developed. It is controlled by an analog-based unit. The main difference between the proposed MPPT system and other systems is that the short circuit current of the pilot-PV module in our system is used to control the DC/DC converter. The circuit of the proposed system does not utilize an expensive digital signal processor nor a microcontroller; hence, the cost and the complexity of the system are reduced.

Key words: Maximum power point tracking, current-based analog MPPT, photovoltaic

1. Introduction

Photovoltaic (PV) energy seems to have an increasing importance as a renewable energy source since it has several advantages, such as it has no noise or moving parts, and it does not need any means of fuel. It has a low maintenance cost and it is environmentally friendly [1].

Despite these advantages, the I-V characteristic of a PV panel is highly nonlinear and changes with irradiance and temperature. There is a unique operating point called the maximum power point (MPP) on the I-V curve of the PV panel, at which the PV panel produces its maximum output power and operates with a maximum efficiency under certain irradiance and temperature conditions. However, since the MPP varies with irradiation and temperature, it is difficult to maintain the maximum power output for all operating conditions. Therefore, MPPT techniques are needed to maintain an operating point of the PV panel at its MPP. Figure 1 shows a block diagram of a common model of an MPPT-based PV system. The MPPT system tunes the voltage and current levels and matches the PV panel to the load.

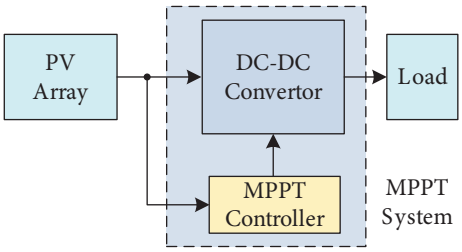

Figure 1. Common model of MPPT-based solar PV system.

To increase the efficiency of PV systems many digital and analog-based MPPT techniques have been developed and reported in the literature. Some examples of the best known are the perturb and observe

*Correspondence: aksoy@cu.edu.tr

(P&O) methods [2,3], the incremental conductance methods (IC) [4,5], the artificial neural network method [6,7], fractional open circuit methods [8,9], fractional short circuit current methods [10], and hybrid methods [11,12]. Detailed reviews of various MPPT systems were given in [13] and [14].

MPPT techniques, which are also called online techniques, utilized in PV systems with different power levels often employ an online seeking algorithm to find the location of the MPP. They maintain the operating point of the PV panel at the MPP using the measured instantaneous value of the PV output voltage, current, and power. Generally, these algorithms used in MPPT techniques perform some complex calculations including multiplication and derivation. Therefore, the complexity of these algorithms requires the use of special processors like a digital signal processor (DSP), a digital signal controller (DSC), or a relatively powerful microcontroller (μC). However, DSPs, DSCs, or μCs and peripheral analog measuring circuits may not be cost-effective for some low power PV applications such as wireless sensor nodes, standalone LED lighting systems, and road traffic signs. In addition, MPPT circuits that contain these devices consume a considerable amount of power. In low power systems, MPPT circuits must have low power consumption since the generated power by the PV panel is low. For this reason, the use of a low cost and low power analog MPPT circuit can be much better and more effective for the low power applications mentioned before [15].

There are several analog-based MPPT techniques in the literature. The analog-based fractional open circuit voltage method is one of the most popular MPPT techniques that utilize an almost linear relationship between the open circuit voltage (V_{OC}) of the PV panel and its voltage at the MPP (V_{MPP}). The relationship between V_{MPP} and V_{OC} can be expressed as $V_{MPP} = k_1 \times V_{OC}$, where k_1 is a proportional constant. Although this method is very simple, it has a major drawback: periodic breaking of the PV panel from the load side for V_{OC} measurement causes a remarkable power loss [10,16]. To overcome this drawback, one pilot cell or module can be used for V_{OC} measurement, but the pilot and the main PV must have the same electrical characteristics [17].

The analog-based fractional short circuit current method exploits the relationship between the current at the maximum power point (I_{MPP}) and the short circuit current (I_{SC}) of the PV panel, which is approximately linear. The relationship between I_{MPP} and I_{SC} can be expressed as $I_{MPP} = k_2 \times I_{SC}$, where k_2 is a proportional constant [14]. This equation shows that I_{MPP} can be determined instantaneously by measuring I_{SC}. Therefore, this method requires a current sensor to measure I_{SC}. To obtain this measurement, it is necessary to create a short circuit condition for the PV panel. It is important to note that no power is supplied to the load by the PV panel during the short circuit condition, which causes a remarkable power loss, just as in the fractional open circuit voltage method. In addition, this measurement also requires a current sensor, which is not cost-effective for a low power PV system.

Various analog-based P&O methods and the ICT have been proposed in the literature [18]. These methods are faster, more accurate, more reliable, and more complex than the fractional short circuit current and the open circuit voltage techniques. They can find the real MPP. However, an analog multiplier and a current sensing circuit are required for the power calculation to implement the analog version of the P&O and ICT. Therefore, these analog-based MPPT systems are complex and uneconomical for low power applications [19].

Another analog-based method is the double linear approximation algorithm (DLAA). The DLAA uses the fact that the locus of the MPP varies nearly linearly with irradiance and temperature. This method requires an irradiance and temperature sensor [20].

In this work, a simple, low-cost, open loop analog-based MPPT circuit with a constant load has been

proposed, simulated, and implemented. The main idea of the proposed technique is based on the tracking of the MPP locus according to the short circuit current of the pilot PV that has different electrical characteristics than the main PV. The proposed system uses a linear relationship between the irradiance and the short circuit current of the pilot PV to find the location of the MPP.

In the proposed method, only the current of the pilot PV is measured while the main PV current measurement is not required. The short circuit current of the pilot PV has a very low DC level without any ripple, so this measurement is made by using a very simple current sensing circuit. Therefore, complex current sensing circuits are not necessary to be designed for the MPPT system.

Popular P&O-based MPPT techniques use searching algorithms [13]. These algorithms cause power losses because of oscillation around the MPP, especially under constant or slow variation of irradiance levels.

The power calculation is not necessary for MPP tracking in the proposed technique. As a result, complex circuits such as samplers and multipliers are not necessary for power calculations.

In addition, the open loop configuration provides a less complex system, which has a low response time for fast changes of irradiance and temperature. Also, this simple analog system has important advantages such as low cost and a reduced PCB size.

This paper is organized as follows: Section 2 describes models of the PV panels. Section 3 explains the theory of MPPT. Section 4 describes the proposed system. Sections 5 and 6 report the simulation results and the experimental results, respectively. Finally, Section 7 contains the conclusion.

2. The models of the PV panels

The equivalent circuit of a single diode model for a single solar cell is shown in Figure 2. The basic equation that describes the I-V characteristic of the PV panel is:

$$I = I_{PH} - I_0 \left[\exp\left(\frac{V + I \times R_S}{n_s V_T} \right) - 1 \right] - \frac{V + I \times R_S}{R_{SH}} \tag{1}$$

where V_T is thermal voltage $\left(V_T = \frac{nkT}{q} \right)$, n is the diode quality factor, n_s is the number of cells, R_S and R_{SH} are the equivalent series and shunt resistance, and I_{PH}, I, and I_0 are the photogenerated current, the panel current, and the saturation current, respectively. Since the saturation current I_0 is very small when compared to the exponential term, '–1' is neglected.

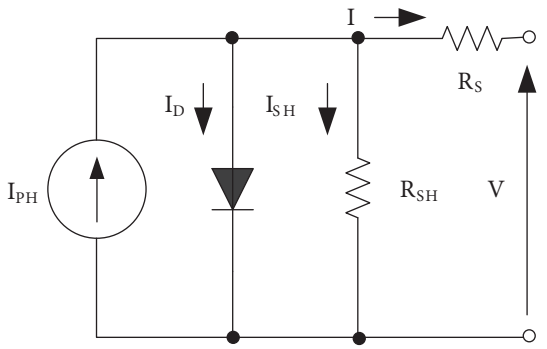

Figure 2. Equivalent circuit of a single solar cell.

The specifications of the PV panel described in the datasheet do not alone provide enough information to construct a single solar cell model. In order to construct a model of the PV panel, five parameters, which

are I_{PH}, I_0, n, R_S, and R_{SH} in Eq. (1), must be determined. These parameters can be determined by using method in [21] and the data from the datasheet of the PV without any measurement. The method in [21] can be explained briefly as follows:

- The short circuit current of the PV, I_{SC}, from Eq. (1):

$$I_{SC} = I_{PH} - I_0 \exp\left(\frac{I_{SC}R_S}{n_s V_T}\right) - \frac{I_{SC}R_S}{R_{SH}} \tag{2}$$

- The current at MPP of the PV panel, I_{MPP}, from Eq. (1):

$$I_{MPP} = I_{PH} - I_0 \exp\left(\frac{V_{MPP} + I_{MPP}R_S}{n_s V_T}\right) - \frac{V_{MPP} + I_{MPP}R_S}{R_{SH}} \tag{3}$$

- The open circuit current of the PV panel, I_{OC}, from Eq. (1):

$$I_{OC} = I_{PH} - I_0 \exp\left(\frac{V_{OC}}{n_s V_T}\right) - \frac{V_{OC}}{R_{SH}} = 0 \tag{4}$$

- The derivative of power with respect to voltage is zero at the MPP:

$$\left.\frac{dP}{dV}\right|_{\substack{V=V_{MPP}\\ I=I_{MPP}}} = I_{MPP} + V_{MPP}\frac{-\dfrac{(I_{SC}R_{SH} - V_{OC} + I_{SC}R_S)\exp\left(\frac{V_{MPP}+I_{MPP}R_S-V_{OC}}{n_s V_T}\right)}{n_s V_T R_{SH}} - \dfrac{1}{R_{SH}}}{1 + \dfrac{(I_{SC}R_{SH} - V_{OC} + I_{SC}R_S)\exp\left(\frac{V_{MPP}+I_{MPP}R_S-V_{OC}}{n_s V_T}\right)}{n_s V_T R_{SH}} + \dfrac{R_S}{R_{SH}}} = 0 \tag{5}$$

- The derivative of the current with respect to the voltage is equal to $-1/R_{SH}$ at short circuit conditions:

$$\left.\frac{dI}{dV}\right|_{I=I_{SC}} = -\frac{1}{R_{SH}} = \frac{-\dfrac{(I_{SC}R_{SH} - V_{OC} + I_{SC}R_S)\exp\left(\frac{I_{SC}R_S-V_{OC}}{n_s V_T}\right)}{n_s V_T R_{SH}} - \dfrac{1}{R_{SH}}}{1 + \dfrac{(I_{SC}R_{SH} - V_{OC} + I_{SC}R_S)\exp\left(\frac{I_{SC}R_S-V_{OC}}{n_s V_T}\right)}{n_s V_T R_{SH}} + \dfrac{R_S}{R_{SH}}} \tag{6}$$

Here, I_{MPP}, I_{SC}, V_{MPP}, and V_{OC} are obtained from the datasheet.

The required parameters (I_{PH}, I_0, V_T, R_S, and R_{SH}) are obtained when these equations are solved using numerical methods provided in MATLAB. V_{OC} and I_{SC} depend on the temperature and I_{SC} depends on the irradiance. Because of this, these dependencies must be included in the PV model. Temperature coefficients, Eq. (7), and Eq. (8) are used to include temperature effect in the models. Irradiance effect is also included in the models by using Eq. (9).

$$V_{OC}|_T = V_{OC} + \alpha_{VOC}\,(T - T_{STC}) \tag{7}$$

$$I_{SC}|_T = I_{SC}\left(1 + \frac{\alpha_{ISC}}{100}\,(T - T_{STC})\right) \tag{8}$$

$$I_{sc}|_G = \left(\frac{G}{G_{STC}}\right) I_{sc}|_{STC}\,,\; I_{ph}|_G = \left(\frac{G}{G_{STC}}\right) I_{ph}|_{STC} \tag{9}$$

Here, G is the irradiance level, and α_{VOC} and α_{ISC} are temperature coefficients of V_{OC} and I_{SC}, respectively.

In this study, the STP005 produced by Suntech was used as the main PV panel and the KXOB22-4X3 produced by IXYS was used as the pilot PV panel. The main PV has 36 series connected monocrystalline cells and provides 5 W peak power at standard test condition (STC). The pilot PV has 20 mm^2 surface area and consists of only 3 series connected monocrystalline cells, which provide 20 mW peak power at STC. Datasheet parameters of both of the PVs are given in Table 1 and the parameters calculated by MATLAB that are required to implement single diode models of the PV panels are given in Table 2.

Table 1. Parameters of the utilized main and pilot PV panels taken from datasheets.

Parameter	Symbol	Main PV	Pilot PV	Units
Maximum peak power	P_{MPP}	5	0.0186	W
Open circuit voltage	V_{OC}	21.6	1.89	V
Short circuit current	I_{SC}	0.32	0.015	A
Voltage @ *Pmpp*	V_{MPP}	17.4	1.50	V
Current @ *Pmpp*	I_{MPP}	0.29	0.013	A
Temp. coeff. of V_{OC}	α_{Voc}	–78	–2.1	mV/K
Temp coeff. of I_{SC}	α_{Isc}	0.17	0.042	mA/K
Panel surface area	S	351	1.08	cm^2

Table 2. Parameters of the utilized main and pilot PV panels obtained by using MATLAB.

Parameter	Symbol	Main PV	Pilot PV	Units
Diode quality factor	n	1.62	1.75	-
Diode saturation current	I_0	0.018	0.172	μA
Photo current	I_{PH}	0.32	0.015	A
Serial resistance	R_S	1.40	3.95	Ω
Shunt resistance	R_{SH}	3659	3267	Ω

After the parameters given in Table 2 are inserted into Eq. (1), the single diode model of the PV is implemented and can be simulated in MATLAB.

3. Maximum power point tracking

3.1. Load matching mechanism

It can be seen from Eq. (1) that the I-V characteristic of the PV is nonlinear and depends on irradiance and temperature. The I − V characteristics and MPPs (as a circle marker on the graph) of the PV panel (STP005) are shown in Figure 3a. The maximum power is obtained at a particular voltage V_{MPP} and current I_{MPP} when the internal resistance of the PV is equal to the load resistance, as shown in Figure 3b. Load resistance at the MPP is called optimal load resistance (R_{OP}). However, if atmospheric conditions, i.e. irradiance and temperature, change but the load resistance of the PV is fixed, the operating point of the PV panel moves away from the MPP and the panel becomes less and less efficient due to load mismatching.

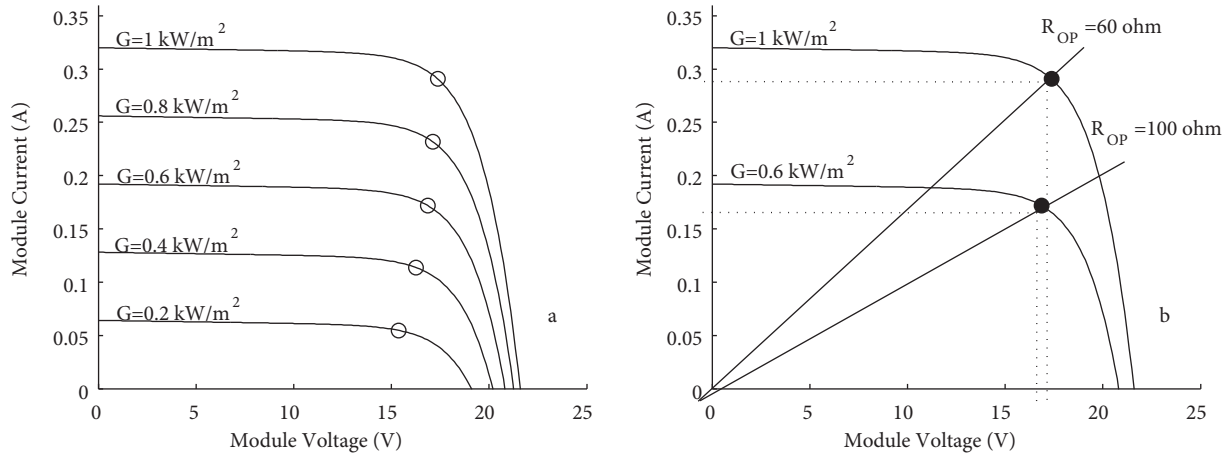

Figure 3. I-V curve of the STP005 at different irradiance levels and load lines (T = 25 °C).

The purpose of MPPT is to maintain the operating point of the PV panel at the highest efficiency point in all operating conditions (irradiance, temperature, and load) by means of adjusting load resistance of the PV. This is achieved with a DC-DC converter. The relationship between input and load resistance of the DC/DC converter can be expressed as:

$$R_{IN} = \frac{R_L}{(M(D))^2} \tag{10}$$

Here, $M(D)$ is the equilibrium conversion ratio (V_{OUT}/V_{IN}) of the converter. Eq. (10) indicates that R_{IN} is a function of R_L and $M(D)$. At the same time, it is clear that for a certain R_L value, R_{IN} can be adjusted by adjusting $M(D)$, which is conversion ratio of the DC/DC converter [22].

4. MPPT system with buck topology DC/DC converter

The relationship between *Irradiance-*R_{MPP} and *Duty-*R_{IN} for the main PV given in Figure 4 was obtained using MATLAB and the PV model carried out as described in Section 2. Figure 5 shows the diagram of a solar panel connected to a DC/DC converter with a buck topology. R_{IN} is the input resistance of the DC/DC converter, which is also the load resistance of the PV panel.

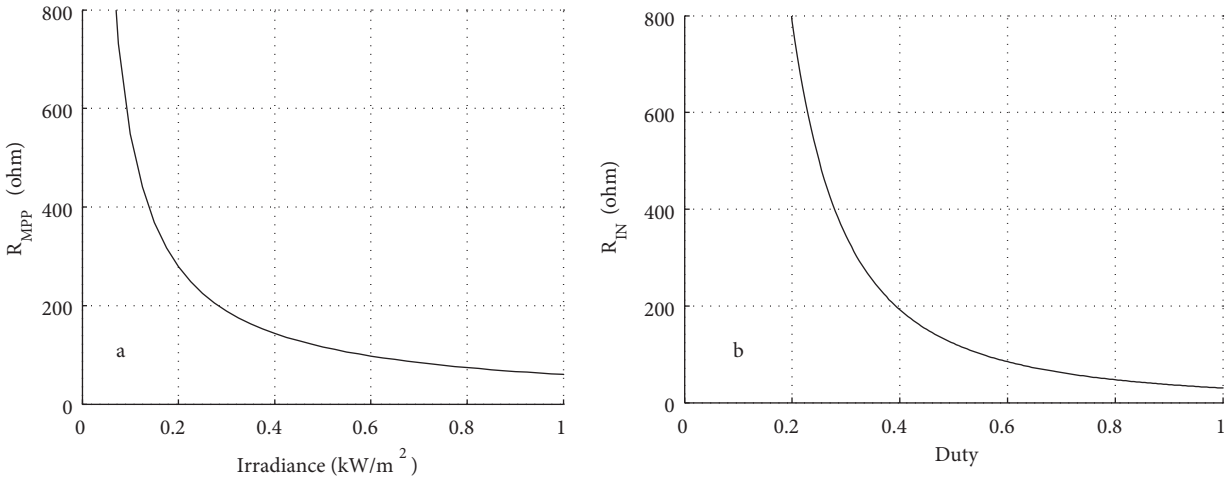

Figure 4. Relationship between *Irradiance-*R_{MPP} and *Duty-* R_{IN} for STP005 PV panel (T = 25 °C).

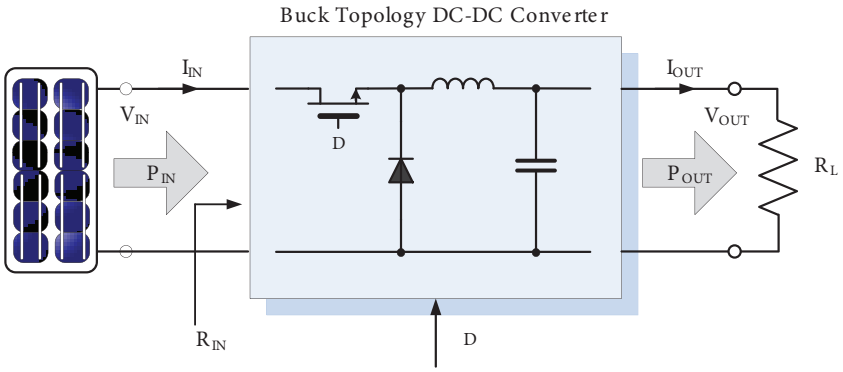

Figure 5. PV module connected to a DC/DC buck converter.

The conversion ratio of the buck topology DC/DC convertor is given as follows:

$$M(D) = D \tag{11}$$

Here, D is the duty cycle of the converter. Putting this in Eq. (10), input resistance of the converter is obtained as:

$$R_{IN} = \frac{R_L}{D^2} \tag{12}$$

Here, D is controlled by a digital or analog-based MPPT system.

5. Proposed system

5.1. Theoretical approach

Figure 4a shows the relationship between irradiance and the load resistance (R_{MPP}) at the MPP for the main PV panel. Figure 4b shows a 30 Ω resistive load (half of the R_{MPP} at STC) connected to the buck topology DC/DC converter's input resistance versus the duty cycle characteristic. As can be seen from Figure 5, R_{IN} is the DC/DC converter's input resistance but also the load resistance of the PV. It is clear that if the duty cycle of the DC/DC converter is adjusted properly according to the R_{MPP} curve, the locus of the MPP can be tracked.

Irradiance $-R_{MPP}$ and *Duty* $-R_{IN}$ relationships given in Figure 4 can be used to obtain the D_{MPP} (duty at MPP) $-$ *Irradiance* relation for the main PV with 30 Ω resistive load connected to the buck topology DC/DC converter. The $D_{MPP}-$ *Irradiance* relationship is obtained using MATLAB and it is shown in Figure 6. Figure 6 shows how the duty cycle (D_{MPP}) of the DC/DC converter should be changed with a given irradiance level for tracking the R_{MPP} curve. It is clear that the irradiance and duty cycle has a nearly linear relationship in the range of 0.2–1 kW/m^2 irradiance level as shown in Figure 6. This linear relationship between irradiance and duty cycle is only valid for the buck topology DC/DC converter. For this reason, a buck converter was used in the proposed system.

On the other hand, the short circuit current I_{SC} varies completely linearly with irradiance as mentioned before. This situation is clearly seen in Figures 7a and 7b, which are drawn for the main PV and the pilot PV, respectively. If the short circuit current of the pilot (I_{SC-P}) is measured and then this value is multiplied by an appropriate constant, the irradiance level of the main PV panel can be obtained and then the obtained irradiance data are used for tracking the R_{MPP} curve of the main PV. This method also does not require

similarities of the short circuit-irradiance characteristics for the pilot PV and the main PV. For this reason, it is not necessary to measure the short circuit current of the main PV (I_{SC-M}).

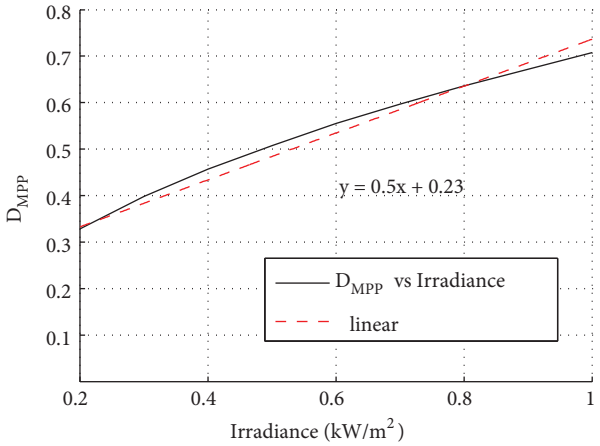

Figure 6. Duty cycle for MPP-Irradiance relationship of the main PV with best fitting line.

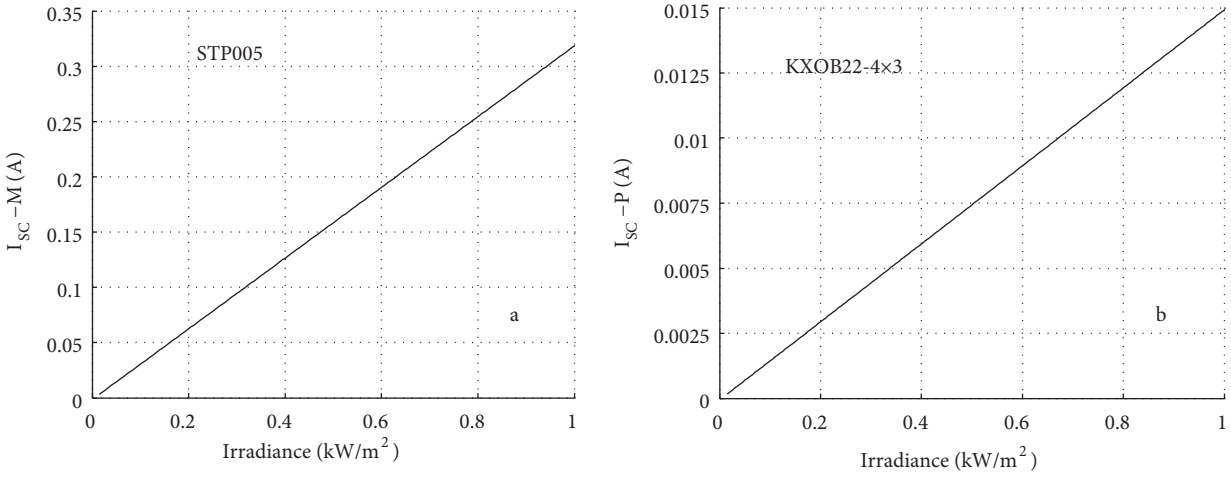

Figure 7. *Irradiance-I_{SC}* characteristics of the main and pilot PV panels.

6. Circuit architecture and implementation

Figure 8 shows the functional block diagram of the proposed analog system. This system consists of five main units, which are the pilot PV, current to voltage convertor (CVC), PWM controller, buck type DC/DC convertor, and main PV. The system operates as follows:

- The I_{SC-P} is multiplied by a constant in order to achieve the main PV irradiance level.
- The scaled I_{SC-P} is sent to an off-set adder in order to obtain I_{SC-M} versus D_{MPP} characteristics given in Figure 6.
- The result of this process produces a control voltage ($V_{CONTROL}$), which is applied to the DC/DC converter as duty cycle control voltage.

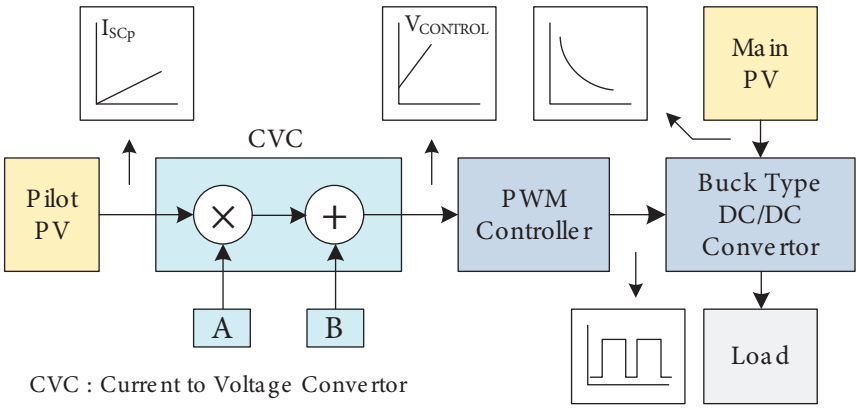

Figure 8. Functional block diagram of the proposed system.

The $V_{CONTROL}$ is expressed as:

$$V_{CONTROL} = A \times I_{SC-P} + B \tag{13}$$

Here, A and B are constants. They are calculated using MATLAB simulation results of the PV panel models and experimental results. These calculations are explained as follows.

Referring to Figure 7b, the relationship between *Irradiance* and I_{SC-P} is written as:

$$I_{SC-P} = 0.015G \tag{14}$$

So, irradiance (G) is expressed as:

$$G = \frac{I_{SC-P}}{0.015} \tag{15}$$

Referring to Figure 6, D_{MPP} is expressed as:

$$D_{MPP} = 0.5G + 0.23 \tag{16}$$

Substituting Eq. (15) into Eq. (16), D_{MPP} is obtained as:

$$D_{MPP} = 33.3I_{SC-P} + 0.23 \tag{17}$$

The TL494 PWM controller control voltage and the duty relation, which is obtained experimentally, are shown in Figure 9. The control voltage of the TL494 is expressed from the best fitting line equation obtained in MATLAB given in Figure 9 as:

$$V_{CONTROL} = 3.023 \times Duty + 0.61 \tag{18}$$

Eq. (17) is substituted in Eq. (18), and then $V_{CONTROL}$ is obtained as:

$$\begin{aligned} V_{CONTROL} &= 3.023(D_{MPP}) + 0.61 \\ &= 99.9I_{SC-P} + 1.3 \end{aligned} \tag{19}$$

Simulation and experimental results give approximately the value of A $=$ 99.9 Ω and the value of B $=$ 1.3 V. Using these results, the CVC is designed with a single supply op-amp (TLC27M4CN) as shown in Figure 10. $V_{CONTROL}$ is used as an input for the PWM converter to control the duty cycle.

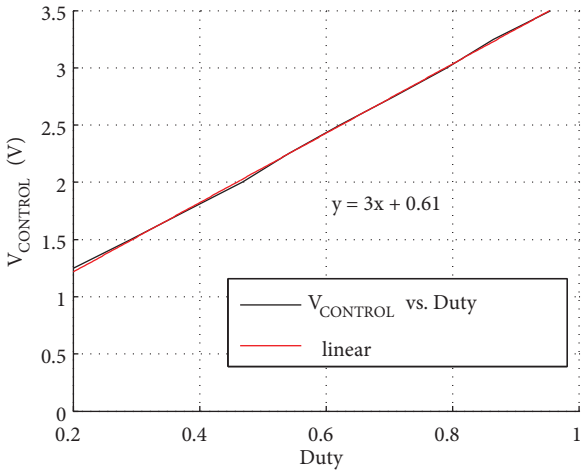

Figure 9. Relationship between duty and control voltage of the TL494 PWM controller with best fitting line.

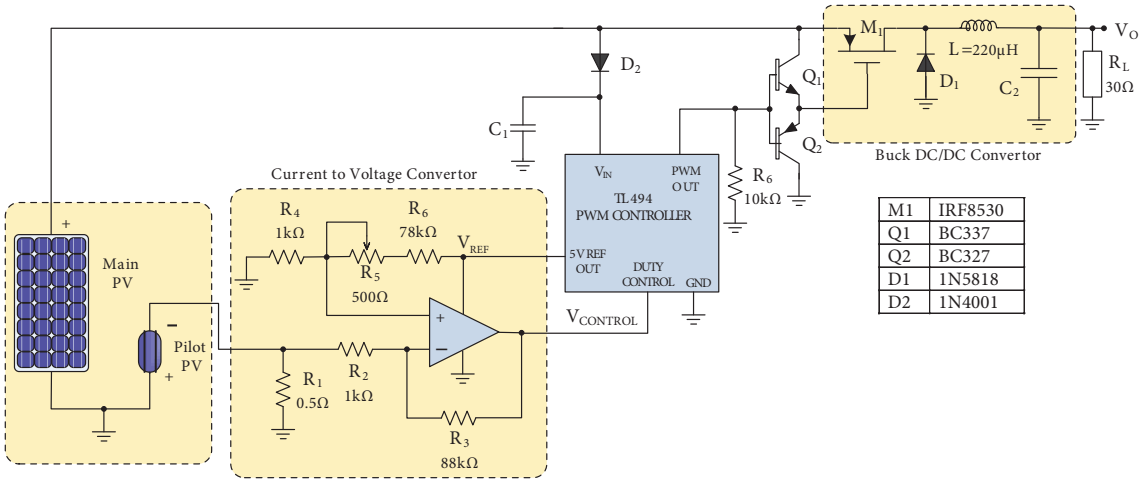

Figure 10. Proposed analog-based MPPT circuit.

The buck topology DC/DC converter is used in the proposed system as shown in Figure 10. Some important design parameters of the implemented buck DC/DC converter are given in Table 3. The buck DC/DC converter switch (M_1) is driven by a commercial PWM controller (TL494).

Table 3. Design parameters of the DC/DC converter.

Parameter	Value
Load resistance	30 Ω
Switching frequency	150 kHz
Inductance, L	220 μH
Output capacitance, C2	100 μF
Input capacitance, C1	470 μF
Load resistance	30 Ω

TL494, which is a PWM controller IC produced by Texas Instruments, has an on-chip oscillator (its frequency can be adjusted by external components), error amplifier, and 5 V precision linear voltage regulator. The precision linear regulator output of TL494, V_{REF}, is used to supply the op-amp circuit.

7. Simulation results

7.1. The PV model verification

The main and pilot PV parameters given in Table 2 are verified in different temperature and irradiance conditions in MATLAB and the simulation results have been compared with the characteristics and values provided by the main and pilot PV datasheets, respectively. The comparison results are given in Figure 11a for different irradiance levels with constant temperature (25 °C) and Figure 11b for different temperature levels with constant irradiance (1 kW/m^2) of the main PV.

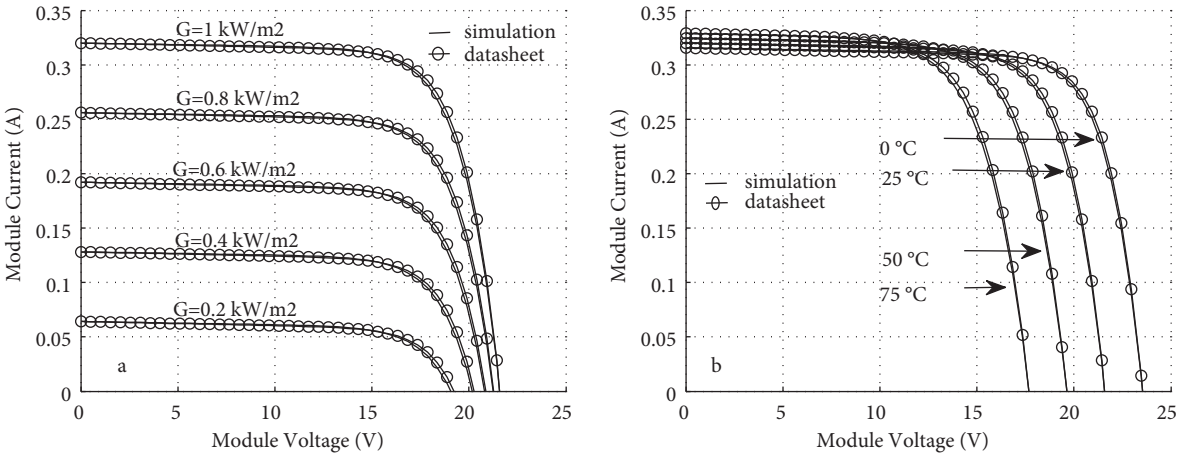

Figure 11. Comparison results of the PV models: (a) at different irradiance and constant temperature (T = 25 °C), (b) at different temperature and constant irradiance (G = 1 kW/m^2).

8. MPPT simulation

Required simulations for verification of the proposed analog MPPT system are made using MATLAB. A flowchart of the MPPT simulation is given in Figure 12. The simulation results of the proposed system under different irradiation and temperature conditions are listed in Tables 4 and 5.

Expected–MP$_{PV}$ is the maximum available power of the PV under given irradiation conditions and at STC temperature. Actual–P$_{PV}$ is the output power of the PV with MPPT system under the same conditions. Both of them are simulation results and obtained using MATLAB. Tracking error, T_e, and tracking efficiency, η_{MPPT}, in the tables are defined as:

$$T_e\% = \frac{\text{Expected } MP_{PV} - Actual P_{PV}}{\text{Expected } MP_{PV}} \times 100$$
$$\eta_{MPPT}\% = \frac{\text{Actual } P_{PV}}{\text{Expected } MP_{PV}} \times 100 \quad (20)$$

As seen from Table 4, η_{MPPT} is greater than 96% for the given irradiance range, which states the effectiveness of the proposed MPPT system. Figure 13a shows output power of the main PV panel when it is connected directly to a 30 Ω resistive load and when it is connected using the proposed MPPT system.

It is clear that while the PV panel has very low operating efficiency without the MPPT system, operating efficiency is very high with the MPPT system, since the proposed system always perfectly tracks the MPP of the PV. Figure 13a shows that the use of the proposed MPPT system can increase the PV output power by as much as 66% for irradiation in the range of 0.2–1 kW/m^2 at 25 °C.

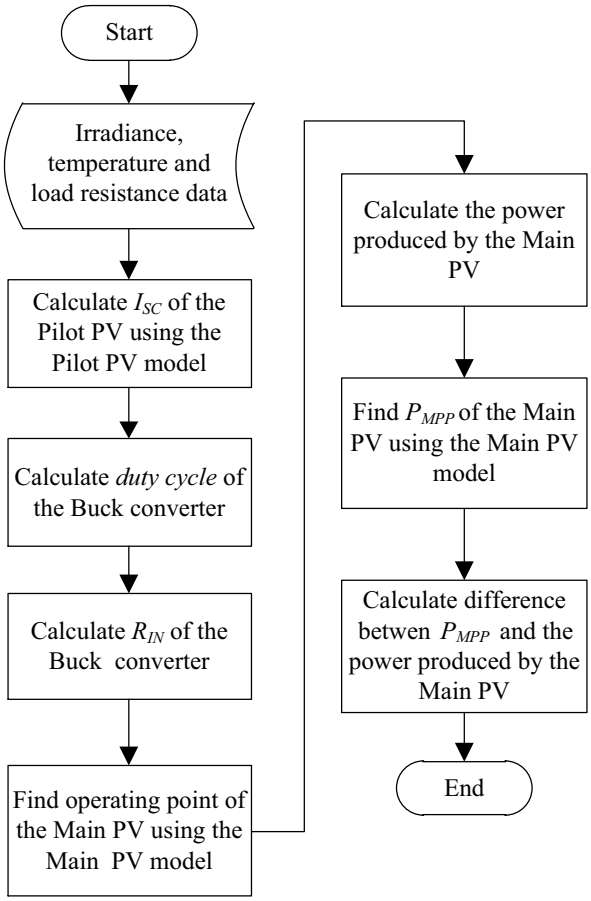

Figure 12. Flowchart of the MPPT simulation.

Table 4. MPPT system error and efficiency at different irradiance levels for T = 25 °C (simulation).

Irradiance (kW/m^2)	Expected MP_{PV} (W)	Actual P_{PV} (W)	Tracking error %	Tracking η_{MPPT} %
0.2	0.84	0.80	3.99	96.01
0.3	1.33	1.33	0.01	99.99
0.4	1.84	1.84	0.48	99.52
0.5	2.37	2.34	0.96	99.03
0.6	2.89	2.86	1.01	98.99
0.7	3.43	3.40	0.76	99.24
0.8	3.96	3.95	0.41	99.59
0.9	4.50	4.50	0	100
1	5.05	5.05	0	100

The simulation results of the proposed MPPT system for different temperature and irradiance levels are given in Table 5. According to Table 5, no significant change is observed in the tracking efficiency when temperature changes.

The simulation results of the proposed MPPT system are compared to the P&O method with fixed step size using real irradiance data provided in [23]. The set of data is the measurements of a cloudy day in April in Barcelona, Spain. The data contain the irradiance measurements taken every 2 min for 12 h. A plot of irradiance versus time is given in Figure 14.

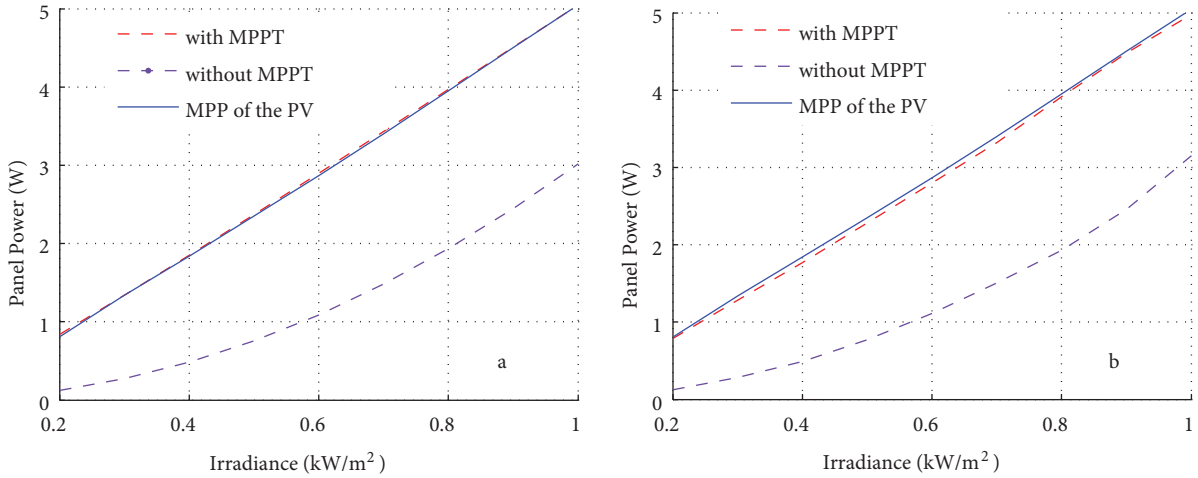

Figure 13. Comparison of output power of the PV with and without MPPT system (simulation and experimental results).

Table 5. MPPT system error and efficiency at different irradiance and temperature levels (simulation).

Irradiance (kW/m^2)	Temp. (°C)	Expected MP_{PV} (W)	Actual P_{PV} (W)	Tracking error %	Tracking η_{MPPT} %
0.5	0	2.65	2.60	1.89	98.11
	25	2.37	2.34	1.27	98.73
	50	2.09	2.06	1.44	98.56
	75	1.80	1.78	1.11	98.89
1	0	5.63	5.62	0.18	99.82
	25	5.05	5.05	0	100
	50	4.47	4.46	0.22	99.78
	75	3.89	3.86	0.77	99.23

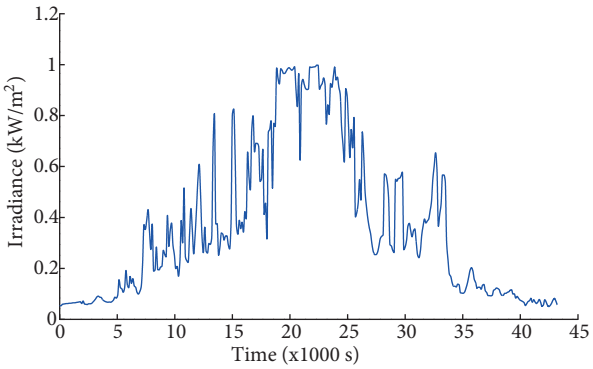

Figure 14. Real irradiance data [23].

Figure 15 shows the comparison results of theoretical (expected) maximum panel power and actual panel powers (P&O and proposed) under real irradiance as given in Figure 14. A part of Figure 15 is given in Figure 16 for detailing the results.

Total electric energy produced by the main PV panel during a 12-h period is calculated using MATLAB with real irradiation data. The results of the proposed and P&O systems are given in Table 6.

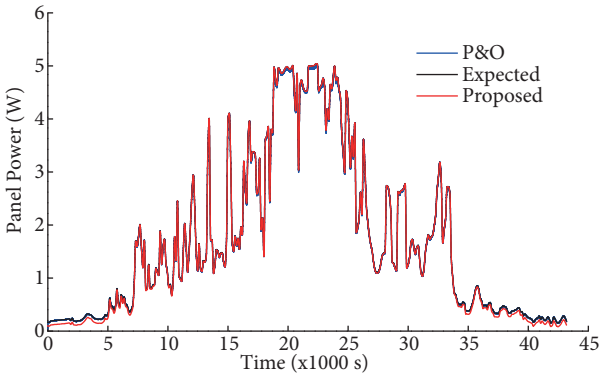

Figure 15. MPPT comparison of the proposed and P&O methods.

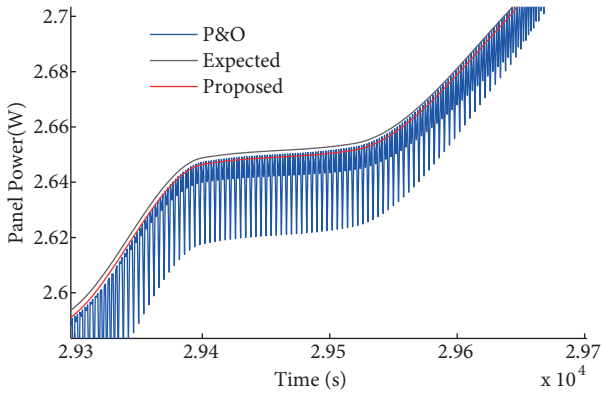

Figure 16. A zoomed section from Figure 15.

Table 6. Daily energy production of the PV panel.

Expected (Wh/day)	Proposed method (Wh/day)	Energy efficiency (%)	P&O method (Wh/day)	Energy efficiency (%)
20.7	20.6	99.5	20.5	99

9. Experimental results

The proposed MPPT circuit was implemented as shown in Figure 17. In order to verify the performance of the proposed system a laboratory implementation is set up and a prototype of the circuit is tested in the laboratory environment. Three Osram HQI-BT (400 W) metal-halide lamps are used to emulate sunlight in laboratory. Several tests have been performed under different irradiance and temperature conditions. Power delivered to the 30 Ω resistive load by direct coupled (without MPPT system) PV system is also measured in order to compare system efficiency. The tracking efficiency for the proposed system is given in Table 7.

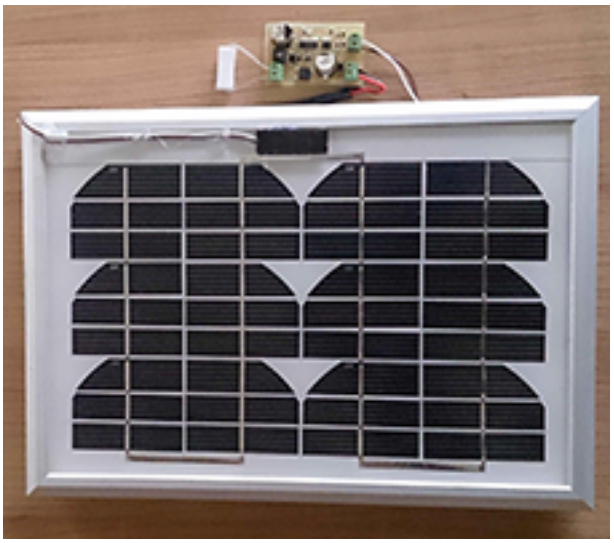

Figure 17. PCB of the proposed system.

Table 7. MPPT system error and efficiency at different irradiance levels for $T = 25\ ^\circ$C (experimental).

Irradiance (kW/m^2)	Expected MP$_{PV}$ (W)	Actual P$_{PV}$ (W)	Tracking error %	Tracking η_{MPPT} %
0.2	0.84	0.79	5.95	94.05
0.3	1.33	1.28	3.76	94.24
0.4	1.84	1.77	3.80	96.20
0.5	2.37	2.28	3.80	96,20
0.6	2.89	2.80	3.11	96.89
0.7	3.43	3.32	3.21	96.79
0.8	3.96	3.91	1.26	98.74
0.9	4.50	4.48	0.44	99.56
1	5.05	4.98	1.39	98.61

In Table 5, minimum tracking efficiency of the proposed system is greater than 94.5%. As can be seen from Figure 13b, the proposed MPPT system can increase delivered power by PV panel up to 63% compared to the direct coupled PV system for irradiation in the range of 0.2–1 kW/m^2 at 25 $^\circ$C. This means that the proposed MPPT system is 63% more efficient than the direct coupled system.

Experimental results that show temperature effect on the MPPT system efficiency are given in Table 8. These results show that maximum deviation of the tracking efficiency due to temperature variation is –3%.

Table 8. MPPT system error and efficiency at different irradiance and temperature levels (experimental).

Irradiance (kW/m^2)	Temp. ($^\circ$C)	Expected MP$_{PV}$ (W)	Actual P$_{PV}$ (W)	Tracking error %	Tracking η_{MPPT} %
0.5	25	2.37	2.28	3.79	96.20
	50	2.09	1.95	6.60	93.40
	75	1.80	1.73	4.14	95.85
1	25	5.05	4.98	1.40	98.60
	50	4.47	4.34	2.91	97.08
	75	3.89	3.80	2.31	97.69

10. Conclusion

In this paper, a new low-cost, open loop analog-based MPPT system without a current sensor that is suitable for low power PV systems has been proposed. The proposed system uses a pilot PV panel as a reference input to adjust the optimum load resistance of the main PV panel. The simulations and the experimental results have demonstrated that the proposed MPPT system can trace the MPP, which significantly increases the efficiency of the PV panel.

There are many problems for conventional current sensing methods, such as the measurement of the high-side PV current, or I_{SC}. Most MPPT systems need complex current sensing circuits. The proposed system, however, does not require any complex current sensing circuit.

On the other hand, the fractional short circuit current method uses the I_{SC} of the PV. The PV must be short circuited during the measurement of the I_{SC}, and meanwhile the generated energy is zero. Also, a large current passes through the MOS switch that is connected to the PV in parallel. Therefore, the efficiency of the MPPT system is reduced. Undesirable conditions are eliminated with the proposed system that uses a very small pilot PV.

As seen in Figure 16, while the P&O method has an oscillation problem around the MPP, the proposed method does not have any oscillation. Because of this oscillation, some amount of energy loss occurs in the P&O methods. In addition, if the atmospheric conditions change quickly, the P&O method takes a considerable time to track the MPP and a significant amount of power is lost during this time [13]. Comparison results given in Figure 15, Figure 16, and Table 6 show that the proposed method eliminates these drawbacks of the P&O methods.

The proposed system does not utilize a DSP, a DSC, or a *mu* C. The circuit of the MPPT system has a very simple analog architecture and it can be implemented easily with low-cost components. The dimensions of the pilot PV utilized in the proposed system are very small in comparison with that of the main PV. Because of the small dimensions of the pilot PV, both of the PV panels can be combined as one single panel.

Another important point that should be emphasized is that the proposed system can easily be produced as a single commercial IC including a PWM controller.

References

[1] Veerachary M, Senjyu T, Uezato K. Voltage-based maximum power point tracking control of PV system. IEEE T Aero Elec Syst 2002; 38: 262-270.

[2] Wasynezuk O. Dynamic behavior of a class of photovoltaic power systems. IEEE T Power Ap Syst 1983; 102: 3031-3037.

[3] Femia N, Petrone G, Spagnuolo G, Vitelli M. Perturb and observe MPPT technique robustness improved. In: IEEE 2004 International Symposium on Industrial Electronics; 4–7 May 2004; Ajaccio, France. pp. 845-850.

[4] Hussein K, Muta I, Hoshino T, Osakada M. Maximum photovoltaic power tracking: an algorithm for rapidly changing atmospheric conditions. IEE Proc-C 1995; 142: 59-64.

[5] Kim TY, Ahn HG, Park SK, Lee YK. A novel maximum power point tracking control for photovoltaic power system under rapidly changing solar radiation. In: IEEE 2001 International Symposium on Industrial Electronics; 12–16 June 2001; Pusan, Korea. pp. 1011-1014.

[6] Hilloowala RM, Sharaf AM. A rule-based fuzzy logic controller for a PWM inverter in a stand alone wind energy conversion scheme. IEEE T Ind Appl 1996; 32: 57-65.

[7] Won CY, Kim DH, Kim SC, Kim WS, Kim HS. A new maximum power point tracker of photovoltaic arrays using fuzzy controller. In: IEEE 1994 Power Electronics Specialists Conference; 20–25 June 1994; Taipei, Taiwan. pp. 396-403.

[8] Schoeman J, Van Wyk J. A simplified maximal power controller for terrestrial photovoltaic panel arrays. In: IEEE 1982 13th Annual Power Electronics Specialists Conference; 14–17 June 1982, New York, NY, USA. pp. 361-367.

[9] Ahmad J. A fractional open circuit voltage based maximum power point tracker for photovoltaic arrays. In: IEEE 2010 2nd International Conference on Software Technology and Engineering; 3–5 October 2010; San Juan, Puerto Rico. pp. 247-250.

[10] Masoum MA, Dehbonei H, Fuchs EF. Theoretical and experimental analyses of photovoltaic systems with voltage and current-based maximum power-point tracking. IEEE T Energy Conver 2002; 17: 514-522.

[11] Adly M, El-Sherif H, Ibrahim M. Maximum power point tracker for a PV cell using a fuzzy agent adapted by the fractional open circuit voltage technique. In: IEEE 2011 International Conference on Fuzzy Systems; 27–30 June 2011; Taipei, Taiwan. pp. 1918-1922.

[12] Weddell AS, Merrett GV, Al-Hashimi BM. Ultra low-power photovoltaic MPPT technique for indoor and outdoor wireless sensor nodes. In: IEEE 2011 Design, Automation & Test in Europe Conference; 14–18 March 2011; Grenoble, France. pp. 1-4.

[13] Esram T, Chapman PL. Comparison of photovoltaic array maximum power point tracking techniques. IEEE T Energy Conver 2007; 22: 439-449.

[14] Faranda R, Leva S. Energy comparison of MPPT techniques for PV systems. WSEAS transactions on power systems 2008; 3: 446-455.

[15] Liu YH, Huang JW. A fast and low cost analog maximum power point tracking method for low power photovoltaic systems. Sol Energy 2011; 85: 2771-2780.

[16] Liu YH, Yang ZZ, Wang SC, Huang JW. A novel analog MPPT technique for low power photovoltaic systems. In: IEEE 2011 TENCON 2011 - IEEE Region 10 Conference; 21–24 November 2011, Bali, Indonesia. pp. 833-837.

[17] Dondi D, Bertacchini A, Brunelli D, Larcher L, Benini L. Modeling and optimization of a solar energy harvester system for self-powered wireless sensor networks. IEEE T Ind Electron 2008; 55: 2759-2766.

[18] Leyva R, Alonso C, Queinnec I, Cid-Pastor A, Lagrange D, Martinez-Salamero L. MPPT of photovoltaic systems using extremum-seeking control. IEEE T Aero Elec Syst 2006; 42: 249-258.

[19] Mattavelli P, Saggini S, Orietti E, Spiazzi G. A simple mixed-signal MPPT circuit for photovoltaic applications. In: 25th Annual IEEE Applied Power Electronics Conference and Exposition; 21–25 February 2010; Palm Springs, CA, USA. pp. 953-960.

[20] Shen C, Tsai C. Double-linear approximation algorithm to achieve maximum-power-point tracking for photovoltaic arrays. Energies 2012; 5: 1982-1997.

[21] Sera D, Teodorescu R, Rodriguez P. PV panel model based on datasheet values. In: IEEE 2007 International Symposium on Industrial Electronics; 4–7 June 2007; Vigo, Spain. pp. 2392-2396.

[22] Erickson RW, Maksimovic D. Fundamentals of Power Electronics. Norwell, MA, USA: Kluwer Academic, 2001.

[23] Castaner L, Santiago S. Modelling Photovoltaic Systems Using PSpice. West Sussex, UK: John Wiley and Sons, 2002.